Supplementary Information for "Competitive interaction of monovalent cations with DNA from 3D-RISM"

George M. Giambaşu[1], Magdalena K. Gebala[2], Maria T. Panteva[1],
Tyler Luchko[3], David A. Case[1] and Darrin M. York[1,*]

August 5, 2015

[1] *BioMaPS Institute for Quantitative Biology and*
Department of Chemistry and Chemical Biology
Rutgers University
174 Frelinghuysen Rd, Piscataway, NJ 08854
[2] *Department of Biochemistry, Stanford University, Stanford, CA 94305 USA*
[3] *Department of Physics & Astronomy, California State University, Northridge, CA 91330*

A Competition of monovalent cations from solving the non-linear Poisson-Boltzmann equation

Solving the conventional non-linear Poisson-Boltzmann equation using software like APBS[5] requires the specification of a single excluding radius. This radius decides how close all the ionic species present in solution can approach the solute and there is no standard way in which the radius should be chosen when cations of different sizes are present in the system. Consequently such calculations cannot distinguish between more or less competitive cations. The competition constant will always be equal to the concentration of the background cation. In the conventional NLPB calculations presented here we have chosen to pick the excluding radius as the size of the background cation so that when the concentration of the competing cation is zero we will obtain the same values for the amount of excess positive and negative charge. Figure 1 presents the ion counting competition profile between K^+ against a background of 50 mM Na^+. Exactly the same profiles were obtained for competition of other cations (Li^+, Rb^+ and Cs^+). Several different variations of NLPB have been suggested[7, 8, 11, 6, 10], that may allow distinction between ions that will effect the competition curves. Nonetheless, as has been demonstrated previously, regardless of how well the profiles for the preferential interaction parameters agree with IC experiments, the fundamental spatial distribution predicted by NLPB are in stark contrast to those predicted from molecular theories such as MD and 3D-RISM[9] (see Figure 15 in supplemental information).

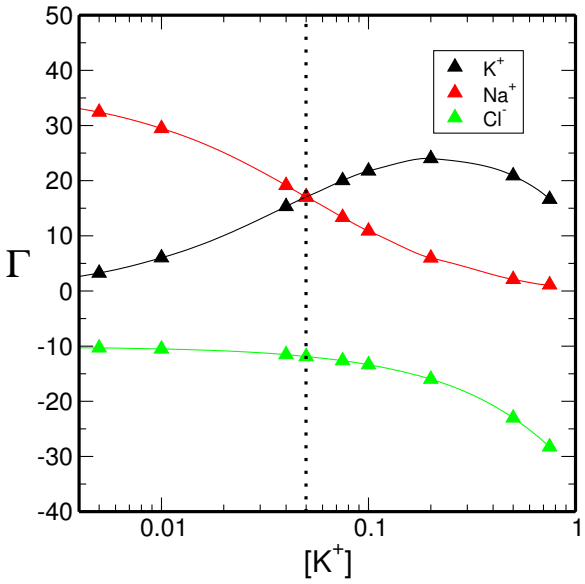

Supplementary Figure 1: Conventional NLPB calculation of the ion counting competition profile of K^+ against a background of 50 mM Na^+.

B A simple model for ion competition

We consider two cations (C^+ and B^+) that compete to be located in the ionic atmosphere of a nucleic acid. We assume that the concentration of B^+ is maintained constant; B^+ will be called the background cation. The concentration of C^+ is varied; C^+ will be designated as the competing cation. A common anion, A^- is used to neutralize the system.

We will consider that a Donnan equilibrium is established between two cells separated by a semipermeable membrane. The cell containing the solution containing the nucleic acid solute is labeled 1 and the cell containing just the salt solution will be labeled 2. All the quantities related to each cell will be henceforth indexed accordingly. Equalization of the chemical potential of the bulk ionic species is written as:

$$\mu^{0,1}_{C^+} + \frac{1}{\beta} ln\gamma^1_{C^+} + \frac{1}{\beta} ln\left[C^+\right]_1 = \mu^{0,2}_{C^+} + \frac{1}{\beta} ln\gamma^2_{C^+} + \frac{1}{\beta} ln\left[C^+\right]_2 \tag{1}$$

An identical relation can be written for B^+ and A^-. μ^0 denotes the standard chemical potential and γ the activity coefficient indexed for each chamber of the osmotic cell and with the corresponding component of the solution; $\beta = {}^1/_{k_B T}$ with T the temperature and k_B the Boltzmann constant. The activity coefficient in the first cell can be separated into a solution part (identical in value to that of cell 2) and an excess part due solely to interactions with the solute. We can write this as a $\gamma^1_{C^+} = \gamma^2_{C^+}\gamma^x_{C^+}$. The smaller the value of $\gamma^x_{C^+}$ the stronger the relative affinity of the cation for the DNA than the solution. Finally, using equation 3 in the main text we replace $\left[C^+\right]_1 = \left[C^+\right]_2 + \Gamma_{C^+}\left[DNA\right]_1$ and obtain:

$$\Gamma_{C^+} = \left\{ \left({}^1/_{\gamma^x_{C^+}}\right) exp\left[-\beta\left(\mu^{0,1}_{C^+} - \mu^{0,2}_{C^+}\right)\right] - 1 \right\} \frac{\left[C^+\right]_2}{\left[DNA\right]_1} \tag{2}$$

The $exp\left[-\beta\left(\mu^{0,1}_{C^+} - \mu^{0,2}_{C^+}\right)\right]$ term can be identified as a transfer equilibrium constant between the solution phase to the ionic atmosphere and will be denoted with K_{C^+}. The $\left({}^1/_{\gamma^x_{C^+}}\right)$ term is concentration dependent and is related to the non-ideality specific to electrolyte solutions. Analogous equations can be derived for Γ_{B^+} and Γ_{A^-}.

Using equation 2, the ratio between the preferential interaction parameters for the competing and background cation can be

computed as:

$$R_+ = \frac{\Gamma_{C+}}{\Gamma_{B+}} = \frac{\left[C^+\right]_2}{c} \tag{3}$$

where

$$c = \left[B^+\right]_2 \frac{\left(1/\gamma^x_{B+}\right) K_{B+} - 1}{\left(1/\gamma^x_{C+}\right) K_{C+} - 1} \tag{4}$$

If one assumes the second term of the rhs to be independent of the concentration of the competing cation, then c is a constant. The validity of this approximation is tested in Figure 2. For competing cation concentrations of up to 100 mM the linear dependence of R_+ holds for both experimental data as well as 3D-RISM.

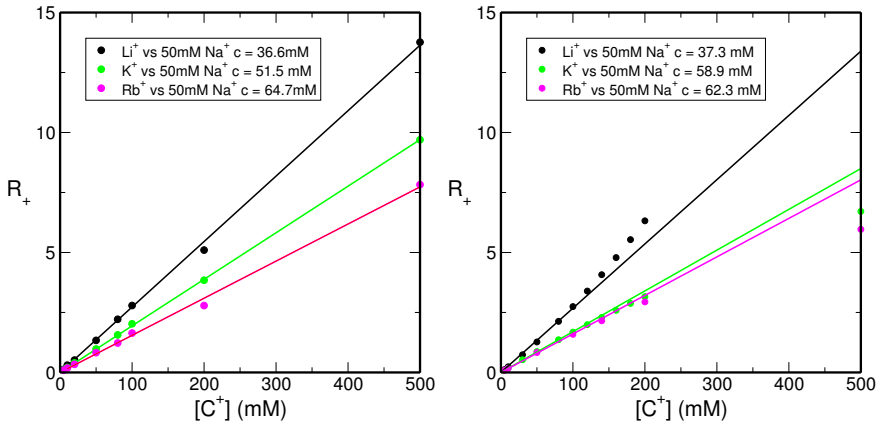

Supplementary Figure 2: R_+ vs competing ion concentration for data collected in [4] (left) and 3D-RISM calculations (right). Fitting of R_+ has been carried out only for the concentrations up to 100 mM and has been extrapolated for the rest of the concentration range.

R_+ can be used to asses the shape of the competition profiles. When the competing and background bulk concentrations are equal ($\left[C^+\right]_2 = \left[B^+\right]_2$), R_+ depends only on the relative free energy of transfer of each cation from bulk to the ionic atmosphere. In general:

1. if $R_+ > 1$, the competing cation is a stronger competitor for the DNA than the background cation. In this case the IC profiles of the background and competing cation intersect before the competing cation concentration reaches the value of the background cation concentration.

2. if $R_+ < 1$, the competing cation is a weaker competitor for the DNA than the background cation. In this case the IC profiles of the background and competing cation intersect after the competing cation concentration reaches the value of the background cation concentration.

The intersection between IC profiles of the competing and background cation can be used to determine the competition constant. In fact, the competing ion concentration where $\Gamma_{C+} = \Gamma_{B+}$ equals the competition constant.

Writing the charge conservation as $q_{DNA} - \Gamma_{A^-} = \Gamma_+$ where Γ_+ is the total excess positive charge, one obtains:

$$\frac{\Gamma_{B^+}}{\Gamma^+} = \frac{1}{1 + \frac{[C^+]_2}{c}} \tag{5}$$

$$\frac{\Gamma_{C^+}}{\Gamma^+} = \frac{1}{1+\frac{c}{[C^+]_2}}$$

The preferential interaction parameters of the competing and background cations normalized by the total positive excess charge (obtained from the ion counting profile of the anion) could be simultaneously fit to experimental or theoretical data for a single parameter, c.

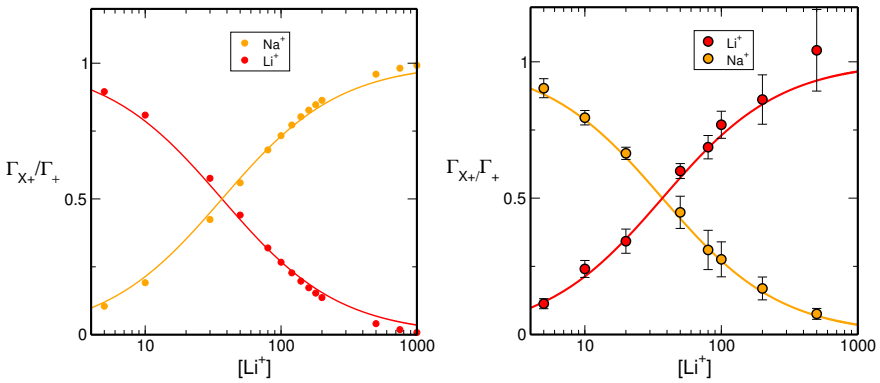

Supplementary Figure 3: Simultaneous fit of 5 to a 3D-RISM derived (left) and experimental (right) competition profile where Li^+ competes against 50 mM Na^+

A linear dependence between the ratio of the number of bound competing and background cation and the ratios of their bulk concentration was also noticed in a previous study on competition between mono- and divalent cations using ASAXS[1] . A similar model to equation 5 was used in [4] to fit experimental data where:

$$\Gamma_{B+} = \frac{\Gamma^{(0)}_{B+}}{1+\left(\frac{[C^+]}{[C^+]_{1/2}}\right)^n} \tag{6}$$

where $\Gamma^{(0)}_{B+}$ is the number of associated B^+ ions in the absence of C^+, and *n* is the Hill coefficient that was found to be very close to 1.0[4], and $[C^+]_{1/2}$ is the competition constant and is similar to parameter c.

C Distribution of cations around phosporyl groups

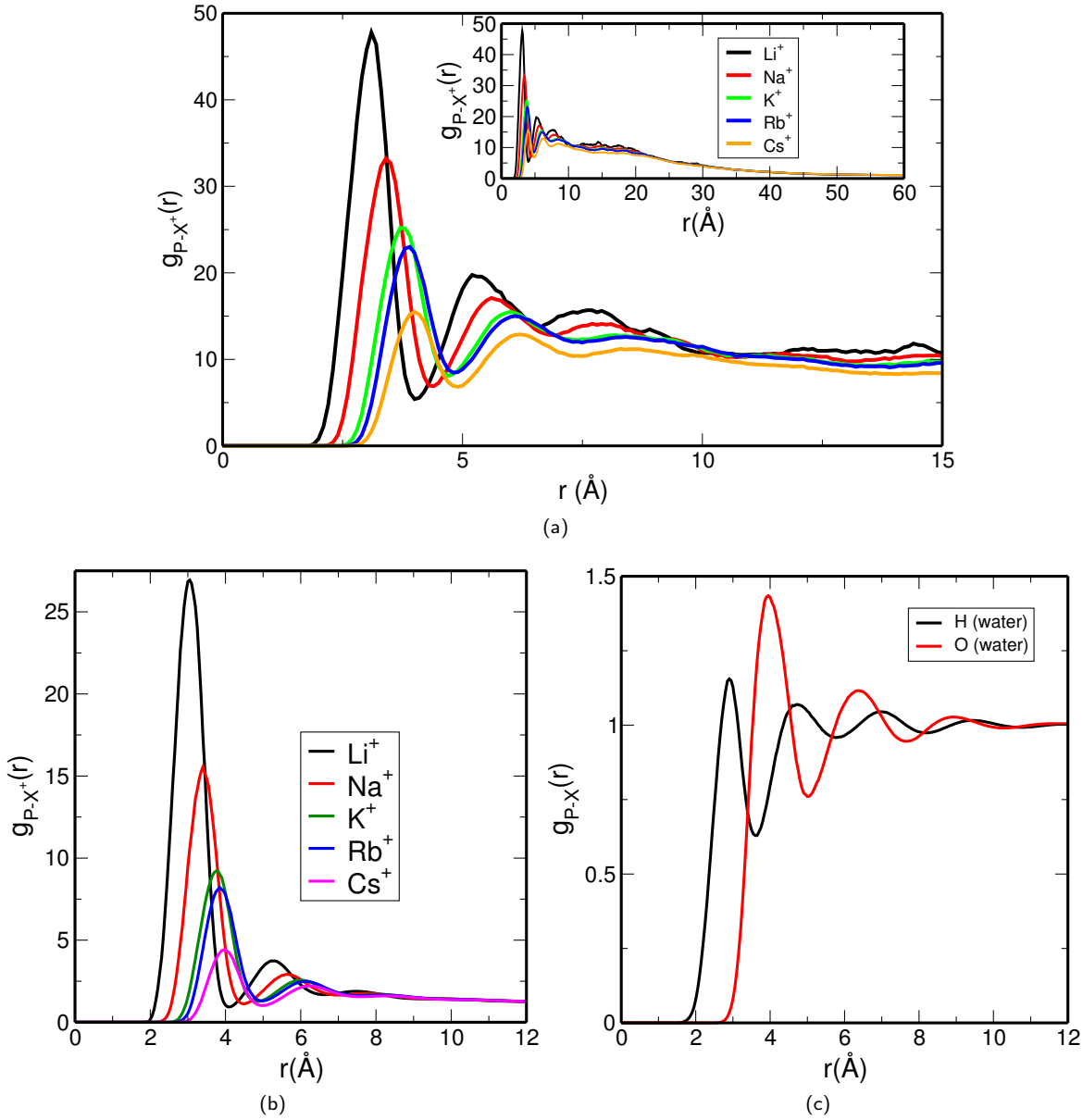

Supplementary Figure 4: Radial distribution functions of alkali cations around a phosphoryl group on the DNA backbone (a) and dimethyl phosphate (b) measured at 50 mM salt (MCl, with M=Li^+, Na^+, K^+, Rb^+, Cs^+) and (c) of water oxygen and hydrogen atoms. The origin of the distribution function is located on the phosphorous atom. A thermodynamic characterization of solvation properties of dimethyl phosphate (excess chemical potential) as a function of salt concentration is provided immediately below.

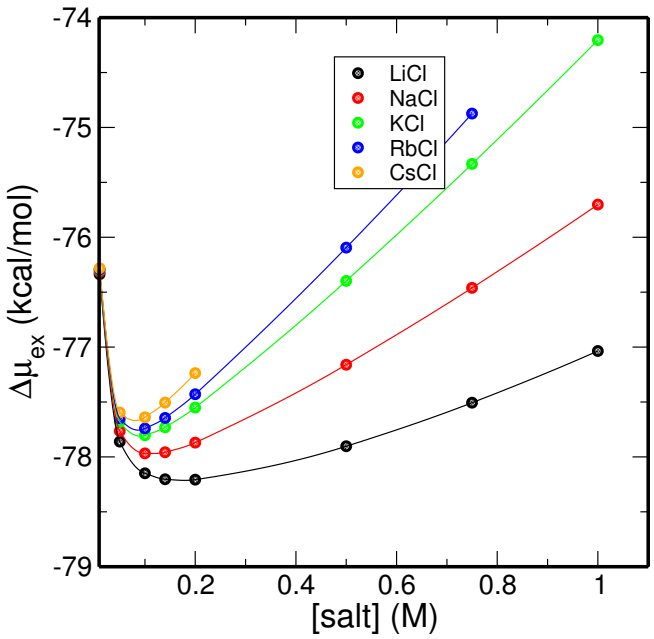

Supplementary Figure 5: Change in the 3D-RISM solvation excess chemical potential of dimethyl phosphate with varying salt concentration.

D Sequence dependence of cation binding to duplex DNA

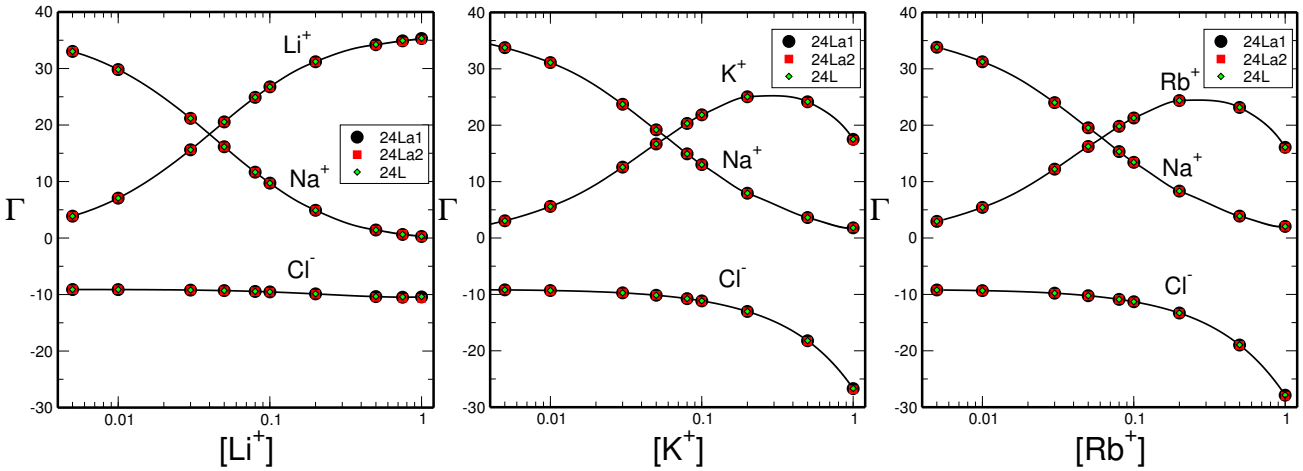

Supplementary Figure 6: Sequence effect on ion counting competition profiles. Overlap of ion counting competition profiles obtained using three different 24bp duplex DNA sequences (24L, 24La1, 24La2). The 24L sequence is shown in green, 24La1 is shown in black and 24La2 shown in red, respectively. The symbols corresponding to each sequence have different sizes to distinguish close numerical values obtained for the three sequences. 24L is the sequence for which most of the ion counting measurements have been carried out; 24La1 and 24La2 correspond to two alternative sequences used in same competition measurements in [4]. See Methods section in the main text for the exact sequences.

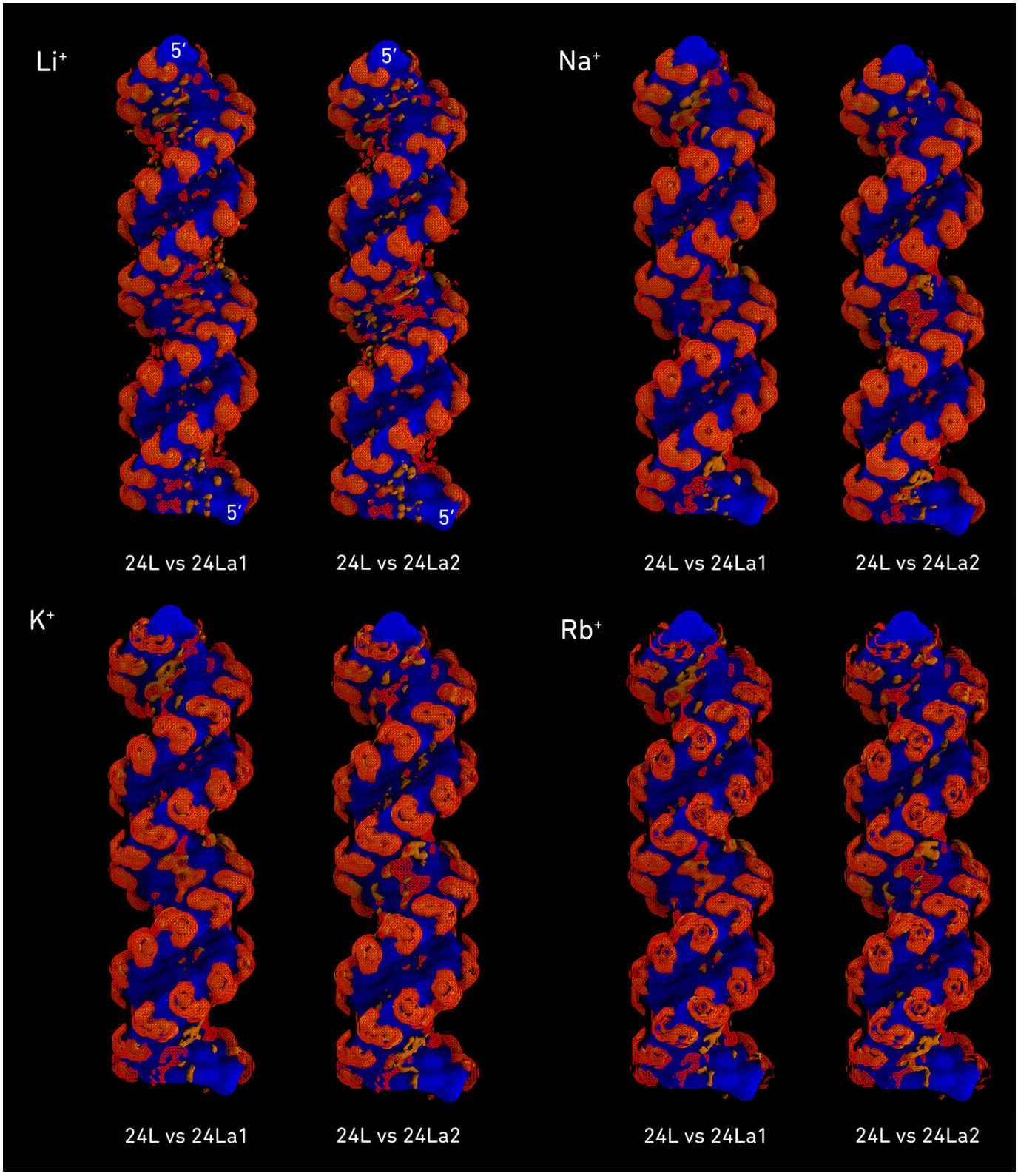

Supplementary Figure 7: Examining the effect of sequence variation on cation binding in the major and minor grooves. Two alternative sequences (See Methods) were used to compute ion competition profiles. The cation iso-density corresponding to the original sequences (24L) is displayed as a red mesh; the cation iso-density corresponding to the alternative sequences (24alt1 left and 24alt2 right) is shown in solid orange. An iso-density value of 50 times the cation bulk concentration has been used throughout.

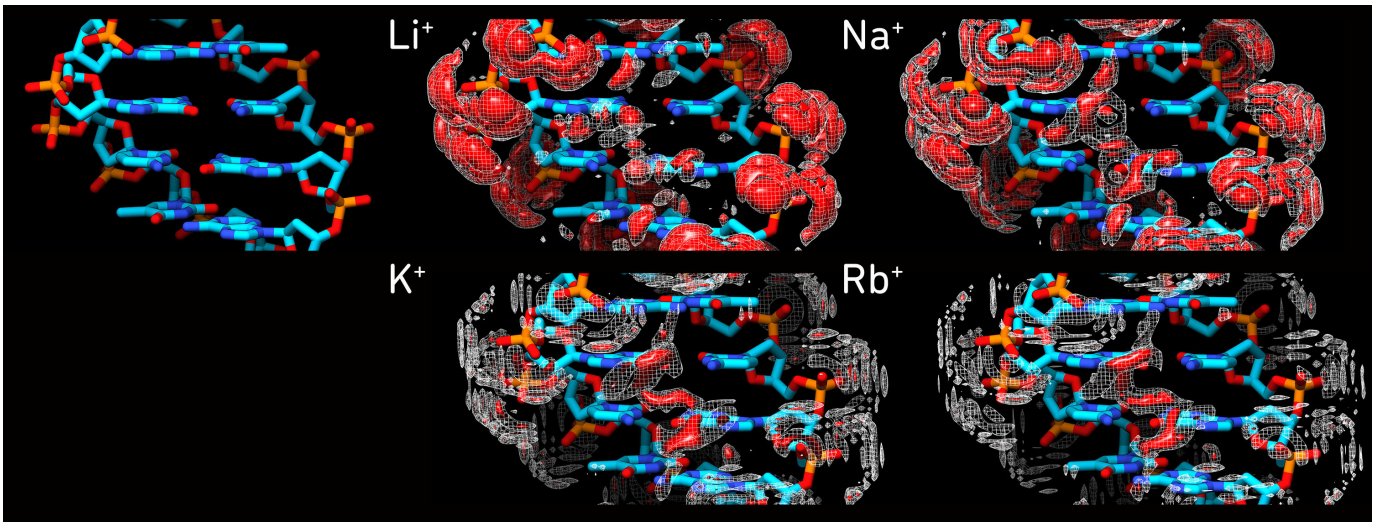

Supplementary Figure 8: Examining ion specific binding in the DNA major groove using the GC/CG base pair step motif. The GC/CG base pair step has been shown using both molecular dynamics simulations and 3D-RISM to chelate Na+ and K+ ions using the O6 atom types on Guanine residues[2, 3, 9]. (top, left) A GC/CG base pair step flanked by two AU base pairs. Ion density iso-value maps for Li^+(top, middle), Na^+(top, right), K^+(bottom, middle) and Rb^+(bottom, right). Two iso-values are shown for each ion type: the white mesh corresponds to an iso-value of 50 times larger than the bulk density, the red solid mesh corresponds to an iso-value of 100 times the bulk ion density. The ion densities presented here were determined for 50mM Li+, K+, Rb+ in the presence of 50mM Na+; the Na+ density shown here was determined at 50mM concentration in the presence of 50mM K+. It can be observed that the cation density patterns both around the phosphoryl groups and the major groove strongly depend on the cation identity.

E Competing cations untwisted densities

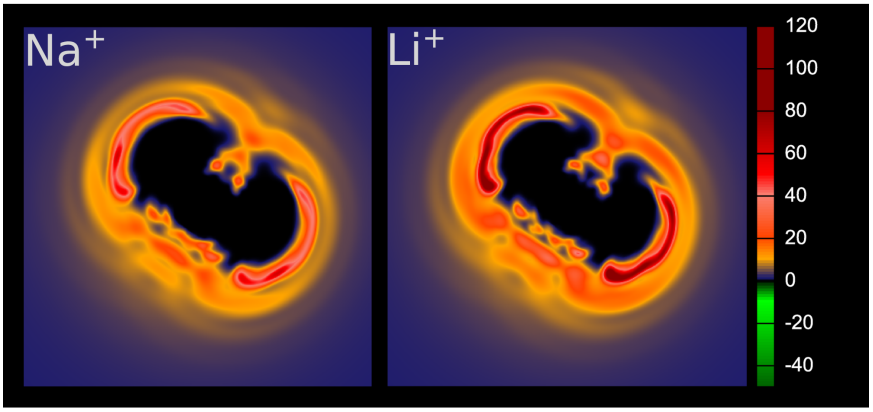

(a)

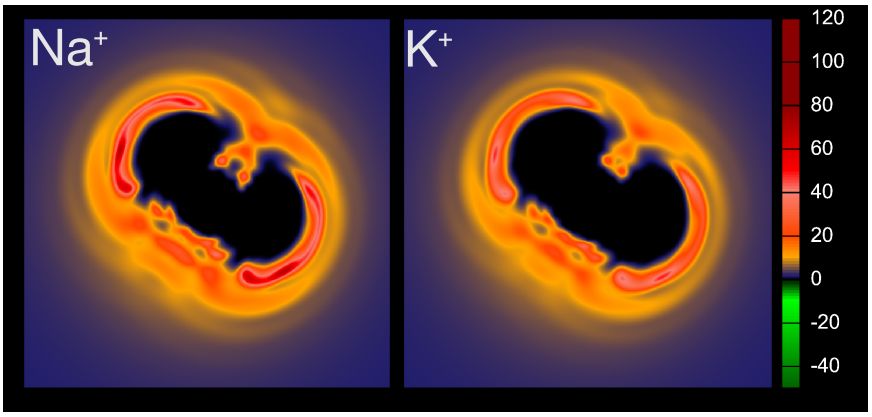

(b)

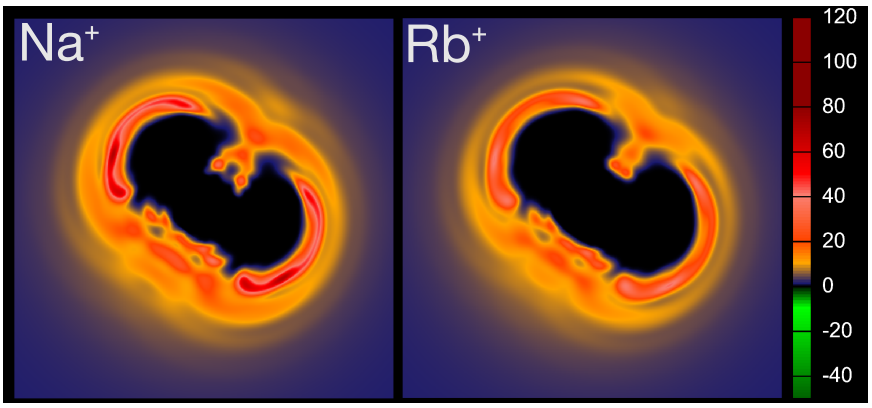

(c)

Supplementary Figure 9: Competing cations untwisted densities. Densities are presented for the case where both cations have the same bulk concentration (50 mM). See main text for the differences between the cations densities (Figure 3).

F Ion counting calculations

[Li^+]	Γ_{Na^+}	Γ_{Cl^-}	Γ_{Li^+}	[Rb^+]	Γ_{Na^+}	Γ_{Cl^-}	Γ_{Rb^+}
0.005	33.00	-9.11	3.87	0.005	33.80	-9.21	2.95
0.010	29.80	-9.12	7.06	0.010	31.30	-9.32	5.42
0.030	21.20	-9.20	15.60	0.030	24.00	-9.78	12.20
0.050	16.20	-9.29	20.60	0.050	19.50	-10.20	16.20
0.080	11.70	-9.43	24.90	0.080	15.30	-10.90	19.80
0.100	9.72	-9.52	26.80	0.100	13.40	-11.30	21.30
0.120	8.26	-9.60	28.10	0.120	11.90	-11.70	22.40
0.140	7.13	-9.68	29.20	0.140	10.80	-12.10	23.10
0.160	6.24	-9.75	30.00	0.160	9.81	-12.50	23.70
0.180	5.51	-9.81	30.70	0.180	9.01	-12.90	24.10
0.200	4.91	-9.87	31.20	0.200	8.33	-13.30	24.40
0.500	1.42	-10.30	34.30	0.500	3.88	-19.00	23.20
0.750	0.64	-10.40	34.90	1.000	2.06	-27.80	16.10
1.000	0.27	-10.40	35.40				
[K^+]	Γ_{Na^+}	Γ_{Cl^-}	Γ_{K^+}	[Cs^+]	Γ_{Na^+}	Γ_{Cl^-}	Γ_{Cs^+}
0.005	33.80	-9.20	3.05	0.005	34.50	-9.27	2.27
0.010	31.10	-9.30	5.59	0.010	32.40	-9.45	4.19
0.030	23.70	-9.72	12.60	0.030	26.30	-10.10	9.53
0.050	19.20	-10.10	16.70	0.050	22.50	-10.80	12.70
0.080	14.90	-10.70	20.30	0.080	18.70	-11.70	15.60
0.100	13.00	-11.10	21.80	0.100	17.00	-12.30	16.80
0.120	11.50	-11.50	22.90				
0.140	10.40	-11.90	23.70				
0.160	9.41	-12.30	24.30				
0.180	8.62	-12.60	24.70				
0.200	7.95	-13.00	25.00				
0.500	3.63	-18.20	24.20				
1.000	1.81	-26.70	17.50				

Supplementary Table 1: Ion counting competition calculations from 3D-RISM for alkali chlorides in a background of 50 mM Na^+. All calculations were carried out using the PSE-3 closure.

References

[1] K Andresen, Rhiju Das, H. Park, H. Smith, L. Kwok, J S Lamb, E. Kirkland, Daniel Herschlag, K D Finkelstein, and L Pollack. Spatial Distribution of Competing Ions around DNA in Solution. *Phys. Rev. Lett.*, 93(24):248103, 2004.

[2] P Auffinger and Eric Westhof. Water and ion binding around RNA and DNA (C,G) oligomers. *J. Mol. Biol.*, 300(5):1113–1131, 2000.

[3] P Auffinger and Eric Westhof. Water and ion binding around r(UpA)12 and d(TpA)12 oligomers–comparison with RNA and DNA (CpG)12 duplexes. *J. Mol. Biol.*, 305(5):1057–1072, 2001.

[4] Y Bai, M Greenfeld, Kevin J Travers, Vincent B Chu, Jan Lipfert, S Doniach, and Daniel Herschlag. Quantitative and comprehensive decomposition of the ion atmosphere around nucleic acids. *J. Am. Chem. Soc.*, 129(48):14981–8, 2007.

[5] N A Baker, David Sept, Simpson Joseph, M J Holst, and J A McCammon. Electrostatics of nanosystems: application to microtubules and the ribosome. *Proc. Natl. Acad. Sci. U. S. A.*, 98(18):10037–10041, 2001.

[6] Alexander H Boschitsch and Pavel V Danilov. Formulation of a new and simple nonuniform size-modified Poisson-Boltzmann description. *J. Comput. Phys.*, 33(11):1152–64, 2012.

[7] Vincent B Chu, Y Bai, Jan Lipfert, Daniel Herschlag, and S Doniach. Evaluation of ion binding to DNA duplexes using a size-modified Poisson-Boltzmann theory. *Biophys. J.*, 93(9):3202–3209, 2007.

[8] Sergei Gavryushov. Electrostatics of B-DNA in NaCl and CaCl2 solutions: ion size, interionic correlation, and solvent dielectric saturation effects. *J. Phys. Chem. B*, 112(30):8955–8965, 2008.

[9] George M Giambau, Tyler Luchko, Daniel Herschlag, Darrin M York, and David A Case. Ion counting from explicit-solvent simulations and 3D-RISM. *Biophys. J.*, 106(4):883–894, 2014.

[10] Robert C Harris, Alexander H Boschitsch, and MO Fenley. Sensitivities to parameterization in the size-modified Poisson-Boltzmann equation. *J. Chem. Phys.*, 140(7):075102, 2014.

[11] Shenggao Zhou, Zhongming Wang, and Bo Li. Mean-field description of ionic size effects with nonuniform ionic sizes: A numerical approach. *Phys. Rev. E*, 84(2):021901, 2011.